

# Atomic Scale Investigations of Transition Metal Dichalcogenides by Scanning Tunneling Microscopy and Atomic Force Microscopy

D. Anselmetti, E. Meyer, R. Wiesendanger and H.-J. Güntherodt  
Institute of Physics, University of Basel, Klingelbergstrasse 82,  
CH - 4056 Basel, Switzerland

F. Lévy and H. Berger  
Institute of Applied Physics, EPFL, PHB - Ecublens,  
CH - 1015 Lausanne, Switzerland

## Abstract

We have studied transition metal dichalcogenides 1T-TiSe<sub>2</sub> and 1T-TaSe<sub>2</sub> with atomic resolution by using scanning tunneling microscopy (STM) and atomic force microscopy (AFM) at room temperature. Besides the investigations of the atomic surface structure, we have studied the charge density wave (CDW) state in the 1T-TaSe<sub>2</sub> compounds by STM. The phasing between the CDW superlattice and the atomic lattice could be determined by imaging both simultaneously. In addition, the CDW modulation is shown to persist right up to surface steps. In contrast to STM, AFM operated with a loading of  $10^{-8}$ – $10^{-7}$  N probes only the atomic surface structure without responding to the charge density wave modulation. Possible explanations for this experimental result will be discussed, including a possible local pressure dependence of the CDW state.

## Introduction

Scanning Tunneling Microscopy (STM) [1] and the later developed Atomic Force Microscopy (AFM) [2] recently opened a new field in physics - the study of solid surfaces in direct space from a submicrometer down to an atomic scale. On the other hand collective phenomena in solid state physics such as charge density wave formation (CDW) have been of great and longstanding interest. The formation and the static structure of CDW's as a consequence of a Fermi surface instability, associated with a periodic lattice distortion (PLD), has been studied by diffraction experiments with electrons, neutrons, X-rays [3] and He-atoms [4, 5]. In contrast to the bulk sensitive methods, the surface sensitive He-scattering experiments have shown, that CDW's propagate up to the crystal surface. Although the scattered He atoms respond to the total charge distribution of a surface, strong superlattice reflections were found due to the CDW modulation.

Transition metal dichalcogenides (TMD) such as TX<sub>2</sub> ( T=Transition Metal, X=S,Se ) are model systems for the possible CDW formation. They are interesting from various points of view. Today it is possible to grow large single crystals, which allow the preparation of large, inert and well defined sample surfaces. Therefore TMD samples are well suited for the investigations by STM and AFM [6, 7], even in air. Previous STM studies of 2H-MoS<sub>2</sub> [8, 9], 2H-NbSe<sub>2</sub> [10], 1T-TaS<sub>2</sub> and 1T-TaSe<sub>2</sub> [11, 12] proved the capability of the STM to image the atomic structure or the CDW superlattice on these materials. Nevertheless it is still not clear whether the imaged atomic structure results from the chalcogen atoms in the top layer [9] or from the electronic d<sub>x</sub>-states of the transition metal atoms in the second layer [8]. The large corrugation heights for the atomic lattice ( $\approx 1$  Å) and the CDW superlattice (2–3 Å) can be explained by a theory of Tersoff [13].

(received October 19, 1989)

The STM technique is known to be sensitive to electronic states near the Fermi energy. On the other hand, the question how one can relate AFM images obtained by the force interaction with the local electronic structure of the sample, is still open. Thus CDW materials with their special electronic structure seem to be very promising for AFM studies.

## Experimental

The STM and AFM are mounted on a commercial antivibration table and work at ambient pressure. The designs of the microscopes are described in previous publications [14, 15]. The tips, acting as sensors in STM, were mechanically prepared or electrochemically etched W, PtIr or Ni wires. In contrast, microfabricated cantilevers with typical spring constants between 0.3–1 N/m were used in the AFM, allowing measurements with a force interaction in the range of  $10^{-8}$ – $10^{-7}$  N by monitoring the deflection of the cantilever with electron tunneling.

Figures 1 and 2 are STM images on  $\text{TiSe}_2$ . The left  $5000 \text{ \AA} \times 5000 \text{ \AA}$  image (figure 1) shows clearly the stepped layer compound structure of these TMD material. Figure 2 shows the same sample on a nanometer scale. The atomic lattice is clearly resolved with defects in the upper right hand part. The lattice constant was determined to be  $3.6 \pm 0.1 \text{ \AA}$ , which agrees well with the known value of  $3.55 \text{ \AA}$  for the bulk.

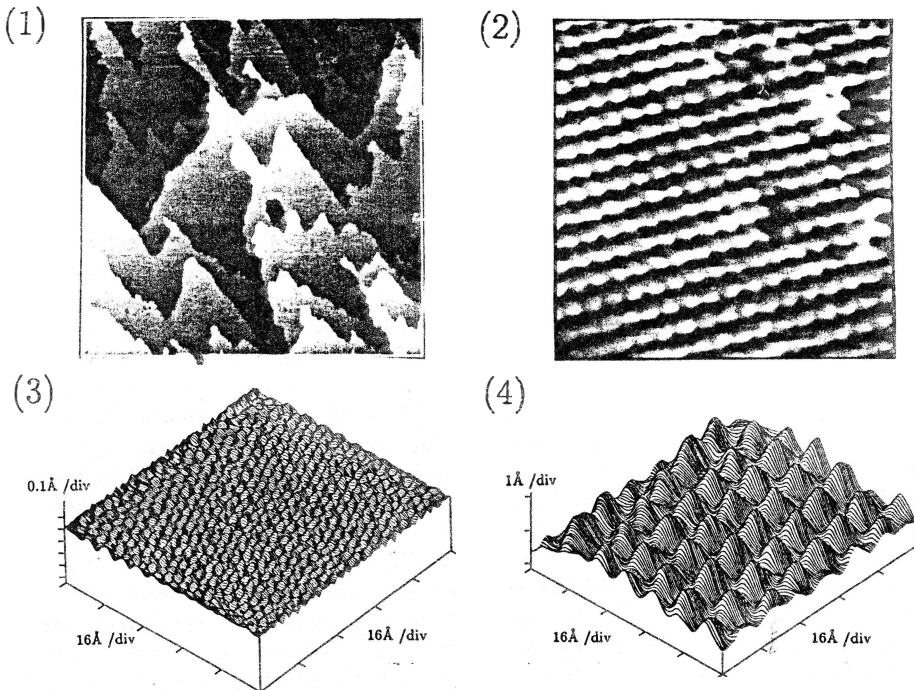


Fig.1: STM topview image of a  $5000 \text{ \AA} \times 5000 \text{ \AA}$  area of  $\text{TiSe}_2$  (Tunneling current  $I_t = 1 \text{ nA}$ , Bias voltage  $U_s = 490 \text{ mV}$ ). The layer compound structure is visible. Fig.2: STM topview image of  $\text{TiSe}_2$  ( $55 \text{ \AA} \times 55 \text{ \AA}$ ,  $I_t = 3 \text{ nA}$ ,  $U_s = 200 \text{ mV}$ ), which shows the atomic structure with a measured lattice constant of  $3.6 \pm 0.1 \text{ \AA}$ . Fig.3: AFM linescan image of  $\text{TaSe}_2$ , showing only the atomic corrugation. The periodicity is  $3.5 \text{ \AA} \pm 0.1 \text{ \AA}$  and agrees well with the atomic lattice constant ( $3.477 \text{ \AA}$ ) of  $1\text{T-TaSe}_2$  ( $80 \text{ \AA} \times 80 \text{ \AA}$ , loading =  $3 \times 10^{-8} \text{ N}$ ). Fig.4: STM linescan image of  $1\text{T-TaSe}_2$  dominated by the  $\sqrt{13} \times \sqrt{13}$  CDW superlattice. ( $80 \text{ \AA} \times 80 \text{ \AA}$ ,  $I_t = 1 \text{ nA}$ ,  $U_s = 30 \text{ mV}$ ).

Images from the CDW system 1T-TaSe<sub>2</sub> are shown in figures 3 and 4. Figure 3 represents an AFM image and figure 4 a STM image of the same size of  $80\text{\AA} \times 80\text{\AA}$ . In the AFM image (figure 3) the atomic lattice with a lattice constants of  $3.5 \pm 0.1 \text{\AA}$  is clearly resolved. The corrugation height is in the range of  $0.3 \pm 0.1 \text{\AA}$  but no evidence of the  $\sqrt{13} \times \sqrt{13}$  CDW superlattice was found, even after fourier transformation of the image.

In contrast, STM images on the same materials are dominated by the CDW superlattice, where the CDW corrugation height is in the order of  $2.5 \pm 0.2 \text{\AA}$ . The observed in-plane lattice constant of  $12.6 \pm 0.1 \text{\AA}$  agrees well with the expected  $\sqrt{13} \times \sqrt{13}$  superstructure (figure 4).

Sometimes STM images show both, the atomic lattice as well as the CDW superlattice (figure 5). The corrugation height in this  $48 \text{\AA} \times 58 \text{\AA}$  image is  $0.8 \pm 0.2 \text{\AA}$  for the atomic structure and  $2.7 \pm 0.3 \text{\AA}$  for the CDW superlattice. The angle between these two lattices was determined to be  $13.9^\circ$ , which agrees well with the values measured from diffraction experiments.

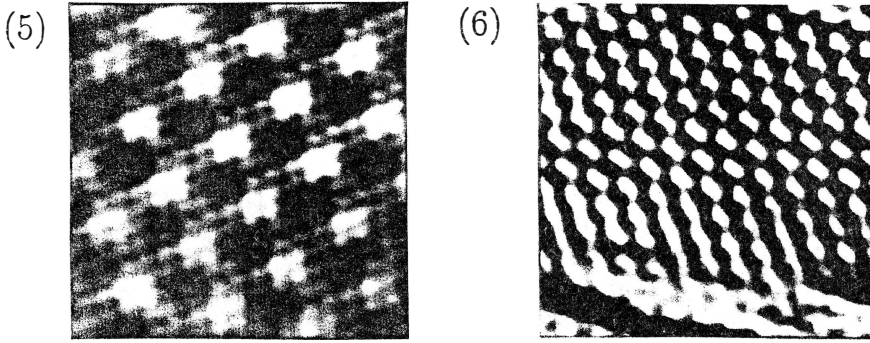


Fig. 5: This STM image of 1T-TaSe<sub>2</sub> shows both the atomic structure as well as the CDW superlattice ( $48\text{\AA} \times 58\text{\AA}$ ,  $I_s = 1\text{nA}$ ,  $U_s = 450\text{mV}$ ). Fig. 6: The STM image of 1T-TaSe<sub>2</sub> (shading processed) shows that the CDW superlattice persists right up to this surface step ( $110\text{\AA} \times 120\text{\AA}$ ,  $I_s = 1\text{nA}$ ,  $U_s = 450\text{mV}$ ).

Furthermore we could find that the CDW superlattice persists right up to defect structures such as steps. The STM picture (figure 6) demonstrates this fact clearly. Additionally a decrease of the CDW corrugation is detectable, which might be characteristic for the decrease of the order parameter near defect structures.

## Discussion

The nonobservance of the CDW superlattice in the AFM experiments is in contrast to STM experiments on these materials, where the image is dominated by the CDW superlattice. STM probes the electronic states near the Fermi energy and should therefore be more sensitive to the CDW states than AFM, which is believed to respond more to the total charge density of a surface similar to the He-scattering experiments. Surprisingly He-scattering experiments on 1T-TaSe<sub>2</sub> at 80 K reveal a corrugation height of  $0.52 \text{\AA}$  for the atomic lattice and the CDW corrugation of  $0.37 \text{\AA}$  which are of the same order of magnitude [4]. Although a reduction of the order parameter at 300 K is expected, it is assumed to be of a small amount because of the high transition temperature in this material ( $T_{trans} \approx 600 \text{K}$ ). A way out of this discrepancy is a presumable difference in the origin of the AFM and He-scattering corrugation, or other mechanisms such as pressure dependence of the CDW state or frictional forces acting during the

AFM experiments.

Transition metal dichalcogenides are highly pressure sensitive. The transition temperatures  $T_{trans}$  of 1T-TaX<sub>2</sub> decrease by an amount of  $dT_{trans}/dp \approx 3-5$  K/kbar [5]. The loading of  $10^{-7}-10^{-8}$  N during AFM investigations is applied on an area of  $\approx 100 \text{ \AA}^2$  and leads therefore to a local pressure of  $\approx 100$  kbar. This might lead a reduction of the transition temperature below room temperature. The final answer to this question can be given by future AFM experiments at lower temperatures and further reduction of the applied loading.

In summary we have shown the capability of STM and AFM to TMD materials from a submicrometer down to an atomic scale. In contrast to STM or He-scattering experiments on 1T-TaSe<sub>2</sub>, which show clearly the CDW superlattice, AFM experiments on 1T-TaSe<sub>2</sub> with loadings in the range of  $10^{-7}-10^{-8}$  N respond only to the atomic modulation.

We would like to thank H.-R. Hidber, R. Schnyder and A. Tonin for technical help. Financial support from the Swiss National Science Foundation and the Kommission zur Förderung der wissenschaftlichen Forschung is gratefully acknowledged.

## References

- [1] G. Binnig, H. Rohrer, Ch. Gerber, and E. Weibel. *Phys. Rev. Lett.* **49**, 57 (1982).
- [2] G. Binnig, C. F. Quate, and Ch. Gerber. *Phys. Rev. Lett.* **56**, 930 (1986).
- [3] J.A. Wilson, F.J. DiSalvo, and S. Manhanjan. *Adv. Phys.* **24**, 117 (1975).
- [4] G. Boato, P. Cantini, and R. Coella. *Phys. Rev. Lett.* **42**, 1635 (1979).
- [5] P. Cantini, G. Boato, and R. Coella. *Physica B* **99**, 59 (1980).
- [6] T.R. Albrecht and C.F. Quate. *J. Appl. Phys.* **62**, 2599 (1987).
- [7] E. Meyer, D. Anselmetti, R. Wiesendanger, H.-J. Güntherodt, F. Lévy, and H. Berger. *Europhys. Lett.* **9**, 695 (1989).
- [8] G.W. Stupian and M.S. Leung. *Appl. Phys. Lett.* **51**, 1560 (1987).
- [9] M. Weimer, J.Kramar, C. Bai, and J.D. Baldeschwieler. *Phys. Rev. B* **37**, 4292 (1988).
- [10] H. Bando, N. Morita, H. Tokumoto, W. Mizutani, K. Watanabe, and A. Homma. *J. Vac. Sci. and Technol. A* **6**, 344 (1987).
- [11] R.V. Coleman, B. Drake, P.K. Hansma, and G. Slough. *Phys. Rev. Lett.* **55**, 394 (1985).
- [12] C.G. Slough, W.W. McNairy, R.V. Coleman, B. Drake, and P.K. Hansma. *Phys. Rev. B* **34**, 994 (1986).
- [13] J. Tersoff. *Phys. Rev. Lett.* **57**, 440 (1986).
- [14] D. Anselmetti, R. Wiesendanger, V. Geiser, H.R. Hidber, and H.-J. Güntherodt. *J. Microsc.* **152**, 509 (1988).
- [15] E. Meyer, H. Heinzelmann, P. Grütter, Th. Jung, Th. Weisskopf, H.-R. Hidber, R. Lapka, H. Rudin, and H.-J. Güntherodt. *J. Microsc.* **152**, 269 (1988).